



1 Totten Ice Shelf history over the past century interpreted from satellite imagery

2

3 Bertie W.J. Miles¹, Tian Li², Robert G. Bingham¹

4 ¹School of GeoSciences, Edinburgh University, Edinburgh, UK

5 ²Bristol Glaciology Centre, School of Geographical Sciences, University of Bristol, Bristol,
 6 UK

7

8 *Correspondence to Bertie.Miles@ed.ac.uk

9

10 **Abstract:** Totten Glacier is currently the largest source of mass loss in the East Antarctic Ice
 11 Sheet and it is projected to be a large source of sea-level rise over the coming century. The
 12 glacier has been losing mass for decades and inland thinning was detected in the earliest
 13 satellite-altimetry observations in the early 1990s, but when the glacier first started losing mass
 14 remains unknown. We calculate decadal ice-speed anomalies to confirm that Totten Glacier
 15 has not undergone sustained acceleration since at least 1973. Together with observations of
 16 grounding-line retreat from 1973-1989, we confirm that the glacier was already out of balance
 17 in the 1970s. Surface undulations form on the Totten Ice Shelf adjacent to an ice rumple near
 18 the grounding line in response to time-varying melt rates and are preserved downstream for
 19 several decades. From utilizing the full suite of Landsat imagery, we produce a century-long
 20 record of surface-undulation formation that we interpret as a qualitative record of basal-melt-
 21 rate variability. An anomalous ~20-year absence of undulations associated with the mid-20th
 22 century manifests a period when ice passing over the ice rumple was pervasively thinner, and
 23 may represent an anonymously warm period that triggered the onset of modern-day mass loss
 24 at Totten Glacier. Our results highlight that the currently available ~30-year satellite altimetry
 25 records are not long enough to capture the full scale of decadal variability in basal-melt rates
 26 and mass-loss patterns.

27 1. Introduction

28 Aurora Subglacial Basin (ASB), located in Wilkes Land, East Antarctica, is drained by five
 29 major outlet glaciers: Holmes, Moscow University, Totten, Vanderford and Denman glaciers
 30 (Fig. 1). Oceanographic observations have confirmed the presence of warm modified
 31 Circumpolar Deep Water (mCDW) on the continental shelf adjacent to each of these outlet
 32 glaciers (Ribeiro et al., 2021; Rintoul et al., 2016; Silvano et al., 2017; van Wijk et al., 2022).
 33 This is accompanied by ongoing grounding-line retreat (Brancato et al., 2020; Li et al., 2023b;
 34 Li et al., 2015; Picton et al., 2023), detachment of the ice shelf from pinning points (Miles and
 35 Bingham, 2024), and ice-front retreat (Baumhoer et al., 2021; Miles et al., 2016) identified
 36 from satellite observations. The rate of mass loss of ASB between 2003 and 2019 is estimated
 37 at -20 Gt yr⁻¹ (Smith et al., 2020), meaning that mass loss from ASB has accounted for just
 38 under 2% of global sea-level rise over this period. Paleo-reconstructions from a variety of
 39 geological evidence show that ASB may have made multi-metre contributions to global sea-
 40 level rise during the warm periods of the mid-Pliocene (Aitken et al., 2016; Cook et al., 2014)



41 when CO₂ concentrations were comparable to the present day (Martínez-Botí et al., 2015).
 42 Therefore, indications from the past and observations of current mass loss suggest that ASB
 43 has the potential to make globally significant contributions to sea-level rise in the coming
 44 decades to centuries (Stokes et al., 2022).

45 Ice discharge from Totten Glacier (Fig. 1) is estimated to be between 65 and 85 Gt yr⁻¹ (Davison
 46 et al., 2023; Rignot et al., 2019), and it is the single largest source of mass loss from both ASB
 47 and the entire East Antarctic Ice Sheet (Mohajerani et al., 2018; Nilsson et al., 2022; Rignot et
 48 al., 2019; Schröder et al., 2019; Smith et al., 2020). Inland thinning of Totten Glacier was
 49 detected in the early 1990s (Nilsson et al., 2022; Schröder et al., 2019), hinting that the
 50 catchment may have been losing mass decades before the earliest satellite-altimetry
 51 observations, but the onset date of this current bout of mass loss is unclear. Recent evidence
 52 shows that enhanced intrusion of mCDW is the most likely forcing of the mass loss at Totten
 53 Glacier. The warm ocean water can flow over the continental shelf (Rintoul et al., 2016) and
 54 travel beneath Totten Ice Shelf towards the grounding line via a network of deep bathymetric
 55 troughs (Hirano et al., 2023), leading to significant basal melting. However, whether and how
 56 this oceanic forcing has varied over time is unknown, and contributing to large uncertainties in
 57 quantifying sea-level rise contributions from Totten Glacier over the coming century and
 58 beyond under a variety of different climate warming scenarios (Jordan et al., 2023; McCormack
 59 et al., 2021; Pelle et al., 2021).

60 Outlet glaciers can lose mass through a dynamical acceleration in ice discharge into the ocean,
 61 a reduction in snowfall, or a combination of both. Unequivocal evidence shows that major
 62 outlet glaciers in West Antarctica that have consistently been losing mass since the onset of
 63 satellite observations are doing so in response to a dynamic-thinning-induced acceleration in
 64 ice-flow speed, forced initially by thinning to the impounding ice shelves (Kim et al., 2024).
 65 However, despite its significant mass loss across the satellite era, existing studies show no clear
 66 widespread acceleration in ice-flow speed across the Totten system (Li et al., 2023a; Li et al.,
 67 2015; Rignot et al., 2019; Roberts et al., 2018). Therefore, the absence of a clear shelf-wide
 68 acceleration at Totten could be explained by two possibilities: 1) Sparse and lower quality
 69 satellite images pre-2000s are not of sufficient quality to capture ice-flow acceleration, or 2)
 70 Totten accelerated before the onset of the satellite era, meaning the Totten catchment was
 71 already out of balance at the onset of satellite observations.

72 Here, we analyse ARGON and Landsat optical imagery to investigate the behaviour of the
 73 Totten glacier and ice-shelf system over the past century. We calculate decadal ice-speed
 74 anomalies and grounding-line migration back to 1973. We also produce a century-long record
 75 of surface-undulation formation that can be taken as a qualitative record of basal-melt
 76 anomalies. We use all three datasets to determine the likely timing for the onset of mass loss at
 77 Totten Glacier.

78

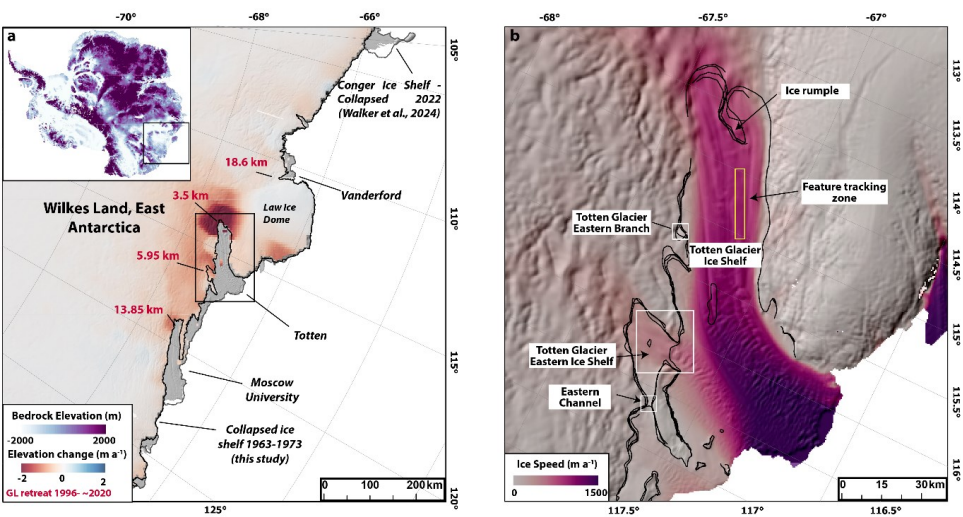
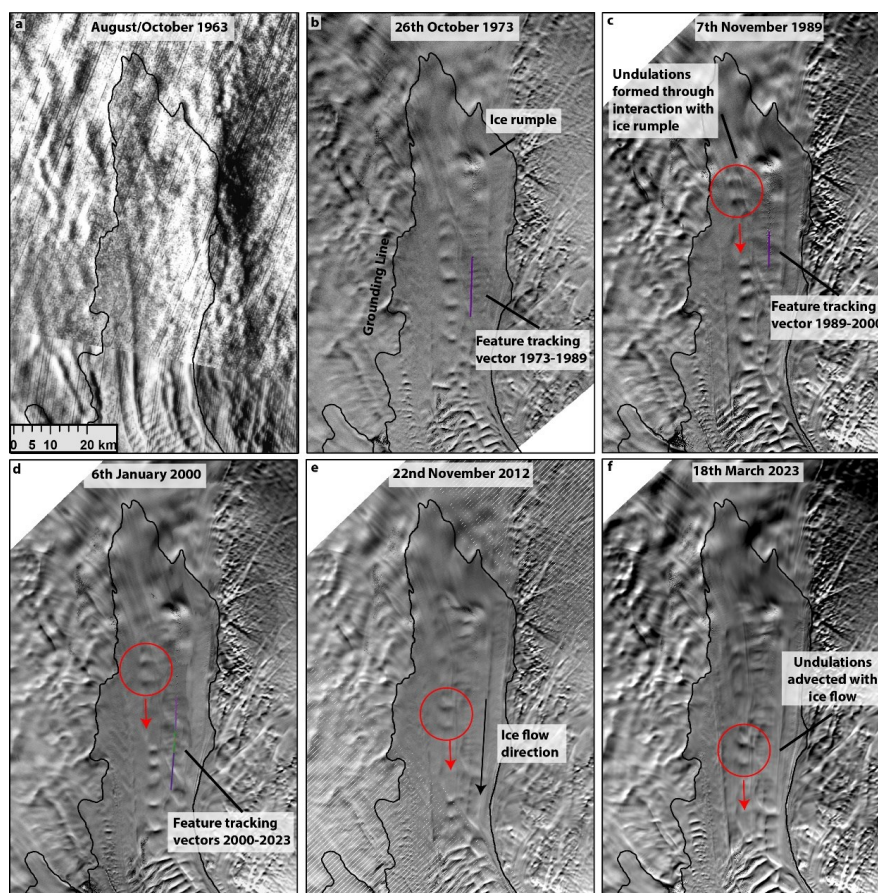


Figure 1: a) Ice-surface elevation change in Wilkes Land, East Antarctica between 2003 and 2019 (Smith et al., 2020), and rate of grounding-line retreat of key outlet glaciers from published studies referenced in the main text. The black line on both images is the MODIS 2009 grounding line (Haran, 2021; Scambos et al., 2007). The inset is bed topography from BedMachine (Morlighem et al., 2020). **b)** Ice speed of Totten system with various InSAR derived grounding lines (Floricioiu, 2021) overlain. The yellow box represents the region of manual feature tracking. The white boxes are the regions where grounding line migration is mapped. The background image in both panels is the REMA DEM (Howat et al., 2019).

2. Methods

2.1 Satellite imagery

The earliest available satellite imagery of Totten glacier system including the ice shelf comprises a pair of ARGON images from 1963 (Fig. 2a). We use the orthorectified and enhanced ARGON imagery of Totten Ice Shelf developed in previous studies (Li et al., 2023a; Ye et al., 2017). The image covering the lower half of the ice shelf and the ice front is of high quality, thus enabling us to identify larger crevasses and surface features. However, the image covering the upper half of the ice shelf and grounding line is of relatively poor quality and the identification of surface features is more challenging (Fig. 2a). For 1973 and 1989, we use the geo-corrected, cloud-free scenes of Totten Ice Shelf acquired respectively by Landsat-1 and Landsat-4 (Miles and Bingham, 2024). Throughout the 2000s, we were able to exploit more regular imagery from Landsat 7, 8 and 9 (Fig. 2). Sporadic SAR imagery is available throughout the 1990s (e.g. ERS), but was not used in this study because we are mainly interested in surface features on Totten Ice Shelf which can express very differently between SAR and optical imagery.



104

105 **Figure 2:** Six decades of satellite imagery over Totten Ice Shelf. The red circles highlight surface
 106 undulations forming near the ice rumple in 1989, before being advected downstream with ice flow.
 107 Feature tracking vectors used to calculate ice-speed anomalies are shown. ARGON (a) and Landsat (b-
 108 f) images are courtesy of the U.S. Geological Survey. Black line shows MODIS 2009 grounding line
 109 (Haran, 2021; Scambos et al., 2007).

110 2.2 Ice Speed

111 Sporadic and lower quality satellite imagery from before 2000 makes it difficult to determine
 112 long-term trends in ice speed at the Totten system. There are two principal reasons for this:
 113 Firstly, post-2000 ice-speed records show large interannual variability, with ice speeds varying
 114 by ~10% over the course of a few years (Greene et al., 2017; Miles et al., 2022). In the absence
 115 of continuous observations in the past, it is difficult to determine whether any apparent changes
 116 in ice speed from isolated observations in the past (e.g. 1973, 1989) are related to long-term
 117 trends or part of this cyclic interannual variability. Secondly, sparse image availability means
 118 that uncertainties can be very high. For example, the only pair of Landsat images covering
 119 Totten Glacier between 1975 and 1998 comprises Landsat-4 images from 28th March 1989 and
 120 7th November 1989. During this relatively short period, ice in the yellow box (Fig. 1b) may
 121 have only flowed ~700 m and, assuming a displacement uncertainty of ± 60 m or 2 pixels (1 for



co-registration; 1 for feature tracking), this equates to uncertainties of around $\pm 9\%$. This very high uncertainty could partly explain the vast range ($>20\%$) of ice-speed anomaly estimates for Totten Glacier in 1989 reported in previous studies (Li et al., 2023a; Li et al., 2015; Rignot et al., 2019; Roberts et al., 2018).

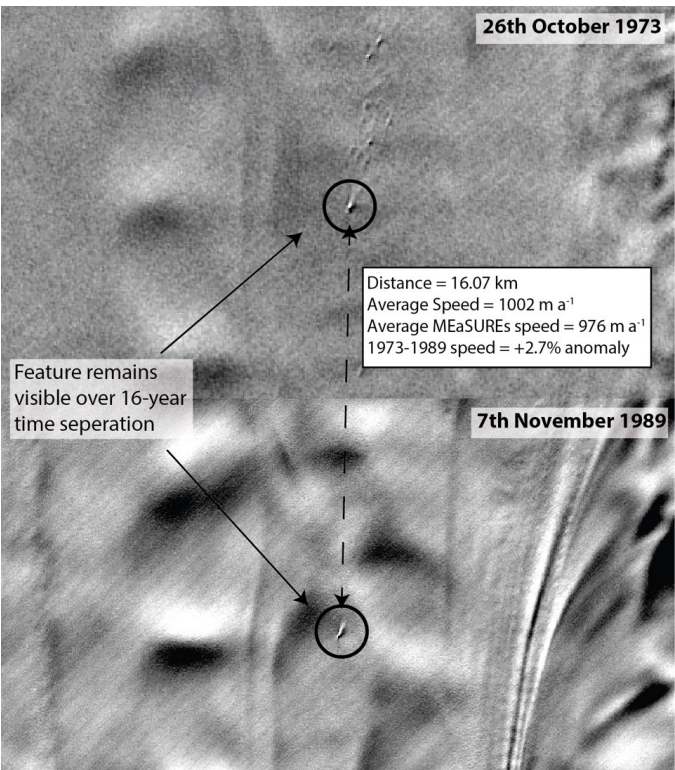
To address both of these issues, we manually track surface features on Totten Ice Shelf using image pairs separated by much longer periods of time (>10 years), which both smooths the impact of interannual variability and reduces relative feature tracking uncertainties because surface features are travelling much greater distances. For example, between 1973 and 1989 we track a 16.07 km displacement of a surface feature and, assuming a displacement uncertainty of two pixels or 120 m (60 m pixel size for Landsat-1), this equates to a smaller uncertainty of $\pm 0.74\%$ (Fig. 3). The disadvantage of this method is that very few surface features remain visible over this length of temporal separation and the process of tracking features over long periods of time can systematically overestimate ice-flow speed if ice does not flow in a straight line (Li et al., 2022). After a careful inspection of the imagery, we focus our feature tracking on one prominent feature that repeatedly forms around 20 km downstream (Location; yellow box, Fig. 1b) of the grounding line, the only feature that unambiguously maintains its shape and structure for multiple decades (Fig. 3). The close proximity to the grounding line of the surface feature and the confined nature of Totten Ice Shelf means the relative speed anomalies likely provide a good proxy for changes in ice speed across the grounding line, as well as the changes in ice discharge of Totten Glacier. Secondly, because ice flows in a straight line in this region, velocity overestimate corrections are not required. We report changes in ice speed in each epoch as an anomaly with respect to the MEaSUREs ice-velocity reference mosaic of Antarctica (Rignot et al., 2011). This is because, in each epoch, the location of the feature that is tracked starts in a slightly different position. All relative anomalies are calculated along the same flowline and the maximum distance between the centre point of any two anomalies is <20 km. Therefore, given their close proximity it is reasonable to infer that the anomalies are closely comparable to each other through time. In total we measure decadal ice-speed anomalies from 10 epochs detailed in Table 1.

Table 1: Feature tracking - decadal ice-speed anomalies

Image 1	Image 2	Days	Distance (km)	Average speed (m a^{-1})	MEaSUREs speed (m a^{-1})	Anomaly (%)	Uncertainty (km)	Uncertainty (%)
26/10/1973	07/11/1989	5856	16.07	1002	976	2.7	0.12	0.75
07/11/1989	06/01/2000	3712	9.54	938	947	-1.0	0.06	0.63
06/01/2000	03/12/2010	3984	10.70	980	974	0.6	0.03	0.28
22/12/2002	22/11/2012	3623	10.01	1008	981	2.8	0.03	0.30
22/11/2006	25/11/2016	3656	10.07	1005	997	0.8	0.03	0.30
09/11/2007	25/09/2017	3608	9.89	1003	999	0.4	0.03	0.30
29/12/2008	17/12/2018	3640	9.98	1001	1005	-0.4	0.03	0.30
14/11/2009	30/08/2019	3576	9.83	1003	1009	-0.6	0.03	0.31
03/12/2010	19/10/2020	3608	9.88	999	1015	-1.6	0.03	0.30
17/11/2013	24/03/2023	3414	8.86	947	959	-1.3	0.03	0.34



151



152

153 **Figure 3:** Image split showing an example of manual feature tracking from a Landsat-1 image from
154 26th October 1973 to a Landsat-4 image from 7th November 1989. Landsat images are courtesy of the
155 U.S. Geological Survey.

156 In addition to decadal ice-speed anomalies, we also calculate interannual ice-speed anomalies
157 at Totten Ice Shelf from 1989 to 2023 where there is a greater availability of satellite imagery.
158 We calculate interannual ice-speed anomalies by manually tracking the same surface feature
159 used in decadal ice-speed anomalies. We chose this method instead of using the existing
160 ITS_LIVE and MEaSUREs annual mosaics because a preliminary analysis showed these two
161 datasets have large differences in the magnitude of ice speed and interannual trends. In total,
162 we measure interannual ice-speed anomalies from 11 epochs detailed in Table 2.

163 **Table 2:** Feature tracking - interannual ice speed anomalies



Image 1	Image 2	Days	Distance (km)	Average speed (m a ⁻¹)	MEaSURES speed (m a ⁻¹)	Anomaly (%)	Uncertain _y (km)	Uncertain _y (%)
28/03/1989	07/11/1989	224	0.69	1124	1004	12.0	0.06	8.70
06/01/2000	22/12/2000	1081	2.76	931	963	-3.3	0.03	1.09
22/12/2000	22/11/2000	1431	3.85	981	971	1.0	0.03	0.78
22/11/2000	29/12/2000	768	2.14	1017	980	3.8	0.03	1.40
29/12/2000	03/12/2001	704	1.98	1029	985	4.5	0.03	1.51
03/12/2001	22/11/2001	720	2.00	1014	1000	1.4	0.03	1.50
22/11/2001	19/10/2001	696	1.85	972	1005	-3.3	0.03	1.62
19/10/2001	25/11/2001	768	2.10	998	1016	-1.8	0.03	1.43
25/11/2001	17/12/2001	752	2.06	1001	1024	-2.2	0.03	1.45
17/12/2001	19/10/2002	672	1.89	1026	1034	-0.8	0.03	1.59
19/10/2002	18/03/2002	880	2.52	1046	1044	0.2	0.03	1.19

164

165 2.3 Grounding Line

166 We use Landsat imagery to map the break-in-slope (Christie et al., 2016; Fricker et al., 2009),
167 a proxy for the grounding-line location. Our analysis is limited to three locations where we
168 observe clear breaks-in-slope, which are the Totten Glacier Eastern Branch, Totten Glacier
169 Eastern Ice Shelf and the Eastern Channel (Fig. 1b). In these regions, break-in-slopes are a
170 good representative for the true grounding line and have been previously used in analysing the
171 basal melting regimes in Totten Ice Shelf due to warm ocean water intrusions (Greenbaum et
172 al., 2015; Li et al., 2023b). We did not map the grounding line at the main glacier trunk of the
173 Totten Ice Shelf featured by fast ice flow, where the break-in-slope is an unreliable proxy for
174 the actual grounding line and the grounding line detection is challenging using DInSAR
175 interferograms or satellite altimetry datasets (Li et al., 2015; Li et al., 2023b). We map the
176 break-in-slope in each location in 1973, 1989, 2000 and 2023. Based on previous studies, we
177 prescribe a mapping uncertainty of 1 pixel (Christie et al., 2016), along with an additional 1
178 pixel uncertainty associated with image co-registration.

179 2.4 Surface Undulations

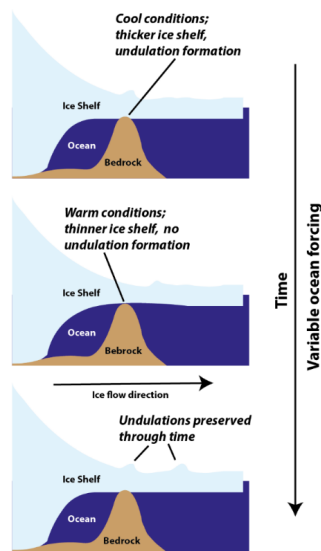
180 Surface undulations downstream of bedrock obstacles on floating ice shelves are common
181 features observed across several ice shelves, with prominent examples expressed on Filchner-
182 Ronne (Brunt et al., 2011), Pine Island (Bindshadler et al., 2011), Thwaites (Kim et al., 2018),
183 Totten (Roberts et al., 2018), and Ross (Lee et al., 2012) ice shelves. As ice flows over bedrock
184 obstacles, the topographic variability of the bedrock surface is transmitted to the glacier surface
185 (De Rydt et al., 2013; Gudmundsson, 2003). If the thickness of floating ice varies over time in
186 response to time-varying basal-melt rates, the degree of contact with the underlying bedrock
187 obstacle will also change, resulting in variable imprints on the surface topography of the ice
188 shelf that are subsequently transported downstream with ice flow (Fig. 4).



189 Sporadic trains of surface undulations form on Totten Ice Shelf adjacent to a large ice rumple
 190 near the grounding line (Roberts et al., 2018); Fig. 2; Animation S1). An inspection of our
 191 cloud-free Landsat imagery spanning 50 years reveals that the trains of undulations persist
 192 relatively unchanged in shape for ~45 km downstream of the ice rumple as they are advected
 193 with ice flow. Therefore, in our earliest cloud-free image from 1973, visible surface
 194 undulations at the furthest point downstream of the ice rumple formed decades earlier and our
 195 full time series provides a near century-long insight into surface-undulation formation.

196 To investigate the surface undulations on Totten Ice Shelf, we first measure surface-elevation
 197 anomalies from ICESat-2 repeat tracks across the ice shelf to capture the dimensions of the
 198 undulations as they are advected downstream with ice velocity (Li et al., 2023b). We use the
 199 ICESat-2 ATL06 dataset for Track 26 between May 2019 and November 2023. The ICESat-2
 200 data are applied using the ‘ATL06_quality_summary’ flag to remove poor-quality elevation
 201 measurements possibly caused by clouds or high surface roughness (Smith et al., 2019). They
 202 are further corrected for the ocean tide and ocean-loading tide, as well as inverted barometer
 203 effects (DAC). Instead of using the ocean-tide correction values generated from the GOT4.8
 204 model that are provided in the ATL06 data product, we use the CATS2008 tidal model to
 205 estimate the ocean-tide corrections (Padman et al., 2002). Elevation anomalies are calculated
 206 by subtracting a reference elevation profile, defined as the average elevation, from each
 207 individual repeat track elevation profile.

208 We then create a time series of surface-undulation formation by estimating the date on which
 209 each undulation formed at the ice rumple. This is estimated by calculating the average flow
 210 speed from the MEaSUREs ice-velocity mosaic of Antarctica along a flowline from the ice
 211 rumple to 45 km downstream, which represents the region where surface undulations are
 212 visible before they are lost to a crevasse field. However, because melt rates are highest near the
 213 grounding line (Adusumilli et al., 2020), it is the cumulative melt as ice travels downstream
 214 from the grounding line that determines the thickness of ice as it flows over the ice rumple.
 215 Therefore, we also estimate the date on which ice flowed over the grounding line by calculating
 216 the average flow speed from the MEaSUREs ice-velocity mosaic of Antarctica along a flowline
 217 from the grounding line to the ice rumple.



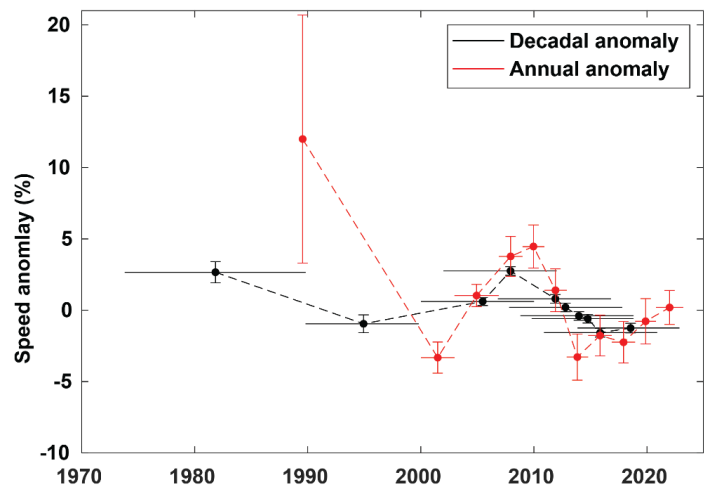
218

219 **Figure 4:** Schematic showing the formation of surface undulations from time-varying melt
220 rates.

221 **3. Results**

222 **3.1 Ice Speed**

223 We observe no clear trend in multidecadal ice-speed anomalies at Totten Ice Shelf between
224 1973 and 2023, with ice-speed anomalies ranging from $-1.6 \pm 0.3\%$ from 2010–2020 to $+2.8$
225 $\pm 0.3\%$ from 2002–2012 (Fig. 5). We observe a much greater range of ice-speed anomalies over
226 interannual timescales. We record a maximum ice speed anomaly of $+12 \pm 8.7\%$ in 1989 and a
227 minimum ice speed anomaly of $-3.3 \pm 1.1\%$ from 2000–2002 (Fig. 5). Regular ice-speed
228 measurements between 2000 and 2023 reveal oscillatory behaviour in speed anomalies of up
229 to $\sim 8\%$ over the course of 6–7 year cycles (Fig. 5).



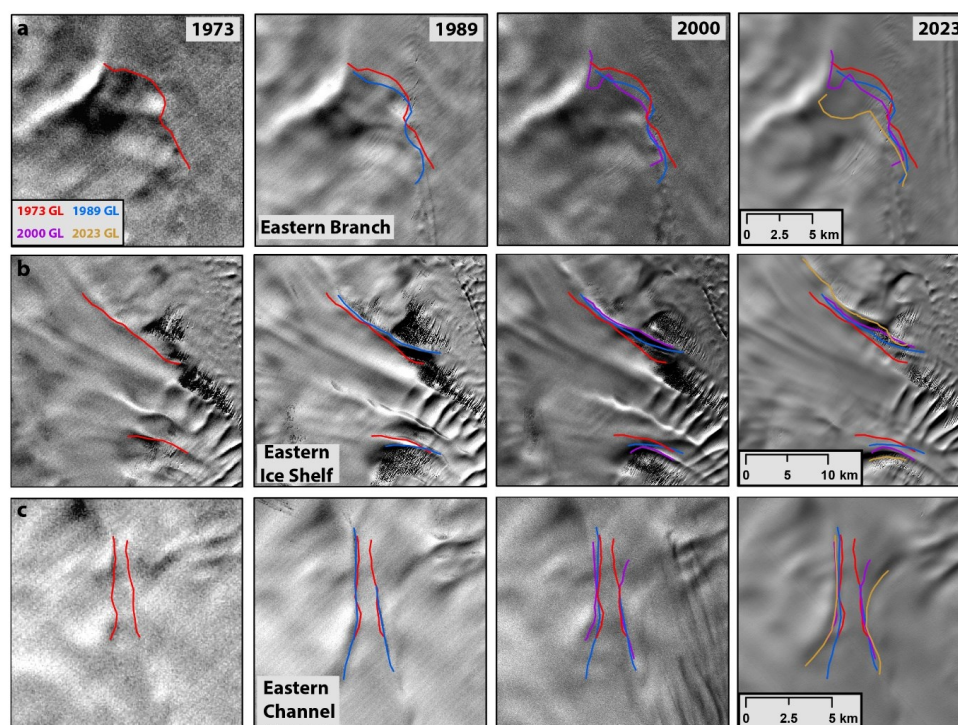
230



231 **Figure 5:** Ice-speed anomalies at Totten Ice Shelf. Black data points represent decadal ice-speed
 232 anomalies; red data points represent the interannual ice-speed anomalies. Horizontal lines represent the
 233 time gap between the two images used to track surface features.

234 3.2 Grounding Line

235 At the Totten Glacier Eastern Branch we observe a maximum 4.1 ± 0.12 km grounding-line
 236 retreat between 1973 and 2023, that includes a 0.8 ± 0.12 km maximum retreat between 1973
 237 and 1989 (Fig. 6a). The width of the mouth of the Totten Glacier Eastern Ice Shelf increased
 238 by around 3.8 ± 0.12 km between 1973 and 2023 with retreat on both the northern and southern
 239 flanks (Fig. 6b). The rate of retreat is reasonably consistent in each of our three epochs: 1973-
 240 1989; 1989-2000 and 2000-2023. At Eastern Channel we observe a gradual widening through
 241 each of our 3 epochs, and overall between 1973 and 2023 the channel width approximately
 242 doubled (Fig. 6c).



243
 244 **Figure 6:** Grounding-line retreat tracked from Landsat imagery for **a)** Eastern Totten Ice Shelf, **b)**
 245 Eastern Ice Shelf and **c)** Eastern Channel. See Figure 1b for locations. Landsat images are courtesy of
 246 the U.S. Geological Survey.

247 3.3 Surface Undulations

248 ICESat-2 repeat tracks across a prominent surface undulation as it flows downstream show a
 249 surface height change of up to 25 m (Fig. 7a). Based on the average flow speed of 950 m a^{-1}
 250 along the transect of the surface undulations, and assuming ice-flow speed has remained
 251 constant through time, the most distant surface undulation 45 km downstream of the ice rumple
 252 will have formed ~ 47 years before the image date (Fig. 7b). We also calculate that it takes



approximately 24 years for ice to flow from the grounding line to the ice rumple based on an average flow speed of 850 m a^{-1} . This means that in our earliest Landsat image in 1973, the most distant surface undulation will have formed in approximately 1926, being imprinted into ice that had crossed the grounding line in approximately 1902 (Fig. 7b). The time series of surface-undulation formation reveals three distinct phases of surface undulation formation over the past 100 years (Fig. 7c). The first phase is characterised by regular surface-undulation formation at the ice rumple between 1926 and 1965, imprinted into ice that had flowed across the grounding line from 1902-1941. The second phase is characterised by a gap in surface-undulation formation between 1965 and 1985, for ice that had flowed across the grounding line from 1941-1961. The final phase is characterised by intermittent formation of surface undulations between 1985 and 2023, imprinted into ice that had flowed across the grounding line from 1961-1999. Notably, surface undulations in this final phase appear to reduce progressively in size, possibly implying a progressive thinning of the ice shelf.

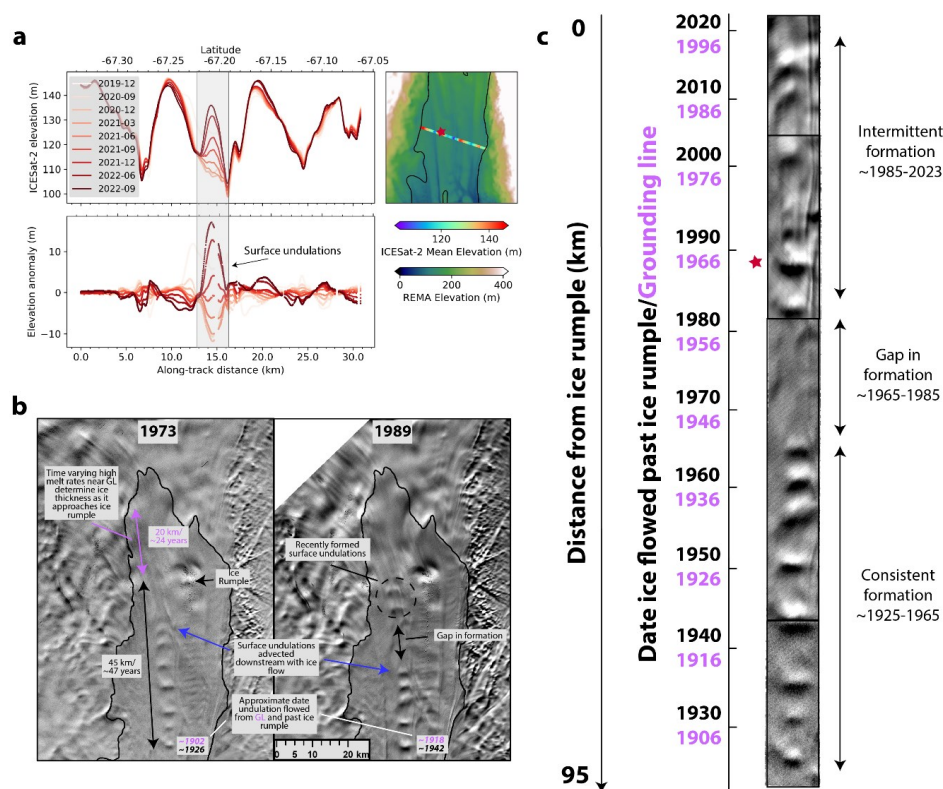


Figure 7: a) Repeat ICESat-2 tracks over Totten Ice Shelf highlighting the surface-elevation anomalies associated with the surface undulations as they flow downstream. Grey box marks the location of the surface undulations and the height change represents the downstream advection of the undulations b) Landsat imagery showing surface-undulation advection downstream. The black line on both images is the MODIS 2009 grounding line (Haran, 2021; Scambos et al., 2007). c) Time series of surface-undulation formation comprised of four Landsat images (1973, 1989, 2000 and 2023) stitched together. The red star represents the surface undulation profile depicted in panel a. Landsat images are courtesy of the U.S. Geological Survey.



275

276 **4. Discussion**

277 **4.1 No speed-up of Totten Glacier since at least 1973**

278 Our results show that there has been no clear multidecadal trend in ice speed at Totten Ice Shelf
 279 from 1973-2023 (Fig. 5). Assuming that ice-speed anomalies in the locations we tracked on the
 280 ice shelf (Fig. 1a) are good proxies for ice speed at the grounding line, this means that average
 281 ice discharge has likely remained relatively unchanged at Totten Glacier over the past 50 years,
 282 despite strong interannual variability. Although there exists some interdecadal variability in
 283 snowfall (Kim et al., 2024), there is no evidence for any long-term trends in snowfall from the
 284 nearby Law Dome ice core (Jong et al., 2022; Roberts et al., 2015) and, because Totten's
 285 present ice discharge outweighs input from snowfall, this means that the Totten catchment was
 286 likely losing a similar amount of mass from 1973-1989 in comparison to the 2000s. Thus, the
 287 trigger for mass loss at Totten catchment predates the onset of the Landsat satellite record.

288 We note that Li et al. (2023a) reported on a long-term speed up at the Totten grounding line
 289 between 1963-1973 and 2022, but with very little change in ice speed 50 km upstream of the
 290 ice front over the same time period (Fig.2; Li et al., 2023a). The rate of acceleration in ice
 291 speed at the grounding line reported in Li et al. (2023a) was not consistent over this time period,
 292 however, with a large ~18% acceleration between 1963-1973 and 1973-1989, then limited
 293 change in ice speed between 1973-1989 and 2022. From our methods, we can only reiterate
 294 that the Totten system has not experienced any multidecadal acceleration since 1973, because
 295 we were unable to track surface features on the 1963 ARGON image near the grounding line.

296 **4.2 Ongoing grounding-line retreat since at least 1973**

297 Our results show consistent grounding-line retreat at Totten Glacier Eastern Ice Shelf and
 298 Totten Glacier Eastern Branch between 1973-1989, 1989-2000 and 2000-2023 (Fig. 6). Our
 299 observation that the grounding line was already retreating in regions where the break-in-slope
 300 is visible between 1973 and 1989 further supports the notion that the Totten Glacier system
 301 was already out of balance and losing mass during this period. The Eastern Channel has also
 302 been consistently widening from 1973-1989, 1989-2000 and 2000-2023 (Fig. 6c). This channel,
 303 first discovered by radio-echo sounding (Greenbaum et al., 2015), has subsequently been
 304 shown to be tidally modulated via satellite-radar interferometry (Li et al., 2023b). The Eastern
 305 Channel is important because it may provide a direct pathway for warm mCDW to enter the
 306 Eastern Ice Shelf cavity (Greenbaum et al., 2015). The expanding width of the channel since
 307 at least 1973 would suggest a greater volume of tidally pumped warm mCDW is being
 308 progressively funnelled through this trough into the ice-shelf cavity.

309 **4.3 Change in melt pattern in the mid-20th century**

310 At Totten Ice Shelf, high basal-melt-rate variability has been observed from autonomous phase-
 311 sensitive radars (Vaňková et al., 2023), variable ocean temperatures have been recorded on the
 312 nearby continental shelf (Hirano et al., 2023; Nakayama et al., 2023; Rintoul et al., 2016), and
 313 variability has been reported in both ice speed (Greene et al., 2017; Miles et al., 2022) and ice-
 314 shelf thickness (Adusumilli et al., 2020; Paolo et al., 2015). The surface undulations that we
 315 have tracked along Totten Ice Shelf are large features that result in up to 25 m differential
 surface-elevation anomalies (Fig. 7a). Roberts et al. (2018) calculated that the wavelength (6-



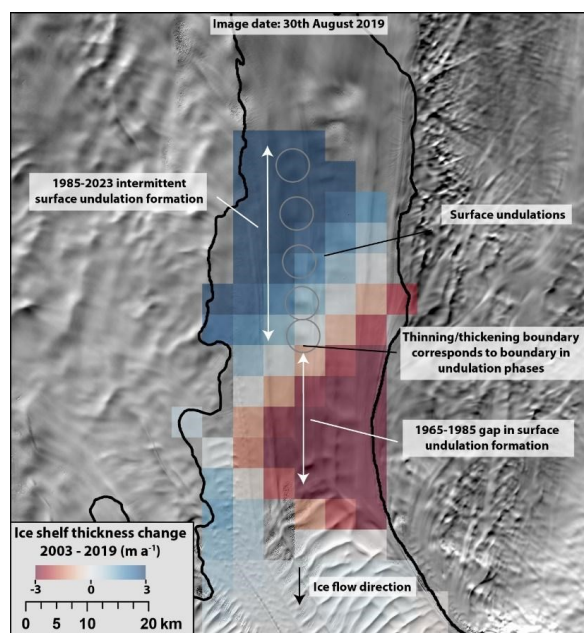
7 years) of the surface undulations in a Landsat-7 image from 2010 matched the wavelength of elevation anomalies of the ice shelf observed from satellite altimetry. We estimate that the average length of all visible surface undulations in Landsat imagery dating back to 1973 is similar, at ~ 5.5 years, based on an average length of ~ 5 km and an average flow speed of 900 m a^{-1} at the ice rumple where the undulations form. Independent ocean modelling has shown the dominant intrinsic variability in the melt rates of Totten Ice Shelf occurs over ~ 3 and ~ 7 years cycles (Gwyther et al., 2018), broadly matching the wavelength of surface-undulation formation. Taken together, along with evidence from similar features on other ice shelves (Bindschadler et al., 2011, Kim et al., 2018), there is substantial theoretical and observational evidence that the surface undulations are formed by time-varying basal-melt rates. Thus, any substantial change in the pattern of surface-undulation formation at Totten Ice Shelf through time likely relates to changes in contact with the underlying pinning point in response to variability in ice-shelf thickness and basal-melt rates.

The abrupt switch from regular surface-undulation formation from 1925-1965 to no surface-undulation formation between 1965 and 1985 implies a change in melt rates and ice-shelf thickness (Fig. 7c). Specifically, because the period from 1965-1985 is characterized by a smoother ice-shelf surface, this suggests warmer conditions and a thinner ice shelf with much more limited interaction with the ice rumple during this period. Surface undulations return sporadically between 1985 and 2023, demonstrating a shift to relatively cooler conditions, but the ice shelf may be thinner compared to 1925-1965 when surface undulations formed on a more regular basis (Fig. 7c).

Modern satellite-altimetry observations of ice-shelf thickness change at Totten Ice Shelf support our hypothesis that the absence of surface-undulation formation between 1965 and 1985 represents a period of higher basal-melt rates and a relatively thinner ice shelf. Observations of ice-shelf thickness change between 2003 and 2019 (Smith et al., 2020) show a conflicting thickness-change signal across the ice shelf (Fig. 8). The upper ice shelf near the ice rumple thickened, while the mid-section of the ice shelf thinned, during this period. This can be explained by waves of ice thickness variations in response to time-varying basal melt rates near the grounding line being advected downstream with ice flow. Notably, the boundary between thinning and thickening ice derived by satellite altimetry (Fig. 8) corresponds to the boundary between the 1985-2023 and 1965-1985 phases in surface-undulation formation (Fig. 7c). That is, the 2003-2019 thickening of the upper section of the ice shelf can be explained by the relatively thinner ice associated with the 1965-1985 period of no surface-undulation formation and high melt rates being advected downstream and being replaced by relatively thicker ice associated with relatively low melt rates and the 1985-2023 period of intermittent surface-undulation formation. The thinning section of the mid-ice shelf is explained by relatively thick ice associated with the 1925-1965 regular phase of surface-undulation formation being advected downstream and being replaced by relatively thin ice associated with the 1965-1985 period of no surface-undulation formation. Therefore, we are confident that the 1965-1985 gap in surface-undulation formation represents a section of relatively thin ice as it flowed over the ice rumple in response to higher basal-melt rates. However, the timing of this period of high melt rates likely predates the 1965-1985 gap in surface-undulation formation. This is because it takes around 24 years for ice to travel from the grounding line to the ice rumple, and it is the cumulative melt rate during this period that determines the thickness of the ice shelf as it crosses the ice rumple. Thus, we estimate that the switch to higher melt rates



362 at the grounding line took place at some point between 1941 and 1965, to which we refer as
 363 the mid-20th century.



364
 365 **Figure 8:** Ice-shelf thickness change between 2003 and 2019 (Smith et al., 2020) overlain on a Landsat-
 366 8 image from August 2019. Black line is the MODIS 2009 grounding line (Haran, 2021; Scambos et
 367 al., 2007). Landsat images courtesy of U.S. Geological Survey.

368 4.4 Warm environmental conditions during the mid-20th century trigger mass loss?

369 We hypothesise that anomalously high basal melt rates in the mid-20th century could have
 370 marked the trigger for the current mass loss of Totten Glacier. This could have manifested via
 371 anonymously warm conditions causing the ice shelf to detach from a pinning point. A candidate
 372 could be the partial detachment from the main ice rumple near the grounding line, where the
 373 precise bed topography is still uncertain (Vaňková et al., 2023). At the very least, the period of
 374 no surface-undulation formation in the mid-20th century likely marked a period of unusually
 375 sustained higher basal-melt rates, with respect to conditions over the past 100 years (Fig. 7c).

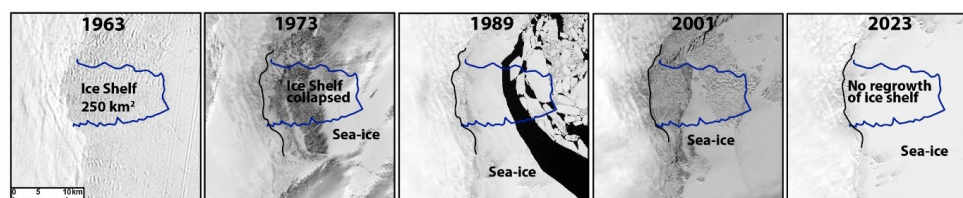
376 The pattern of surface-undulation formation over the past 100 years also supports the notion of
 377 a long-term thinning of Totten Ice Shelf since the mid-20th century. Following the period of
 378 regular surface-undulation formation in the first half of the 20th century, surface undulations,
 379 despite some decadal variability, progressively become less frequent and visibly smaller in size
 380 (Fig. 7c). We interpret this as a long-term thinning of the ice shelf in response to increased melt
 381 rates, meaning increasingly more extreme cold anomalies are required for undulation formation.
 382 This is consistent with ship-based observations of ocean temperature that show a warming of
 383 CDW at the continental shelf adject to Totten Glacier between 1930-1990 and 2010-2018, in
 384 response to a wind-driven southward shift of the Antarctic Coastal Current (Herraiz-
 385 Borreguero and Naveira Garabato, 2022; Yamazaki et al., 2021). However, superimposed on
 386 this longer-term trend of CDW warming are the processes that modulate the delivery of mCDW



387 onto the continental shelf and then towards ice-shelf cavities that are an important factor in the
 388 observed decadal variability in melt rates (Adusumilli et al., 2020; Roberts et al., 2018) and
 389 subsequent surface-undulation formation (Fig. 7c). In the case of Totten Glacier and Ice Shelf,
 390 several processes have been put forward to explain decadal variability in melt rates including
 391 variations in Antarctic Slope Current strength (Nakayama et al., 2021), intrinsic variability
 392 (Gwyther et al., 2018), zonal wind strength on the continental-shelf break (Greene et al., 2017)
 393 and coastal-polynya activity (Gwyther et al., 2014; Khazendar et al., 2013).

394 Validating the hypothesised period of anonymously warm conditions in the mid-20th century
 395 with reanalysis data is challenging. Outputs from ice-ocean models reconstructing temporal
 396 variability in basal-melt rates back to the mid-20th century show conflicting signals (Gwyther
 397 et al., 2018; Kusahara et al., 2024), and the reliability of key climatic reanalysis input data
 398 throughout much of the early to mid-20th century is unknown. There is also a poor
 399 understanding of the sub-ice-shelf bathymetry that is crucial to simulating melt rates (Kusahara
 400 et al., 2024). However, modern observations show synchronous ice-speed and ice-shelf
 401 thickness anomalies throughout the 2000s at major outlet glaciers across the wider Wilkes Land
 402 region (Miles et al., 2022). Therefore, any anonymously warm conditions in the mid-20th
 403 century could have been felt regionally and not just at Totten Glacier. We observe the collapse
 404 of a previously unreported ice shelf 50 km east of the ice front of Moscow University Ice Shelf
 405 between 1963 and 1973 (Fig. 9). The ice shelf is small (250 km²) and did not buttress any large
 406 glaciers, so its collapse is inconsequential for sea-level rise. The unnamed ice shelf was
 407 previously adjoined to Voyeykov Ice Shelf through a mixture of fast ice and melange.
 408 Voyeykov Ice Shelf periodically collapses and regrows in response to changes in fast ice
 409 conditions (Arthur et al., 2021), but at the unnamed ice shelf we observe no signs of regrowth
 410 in the following 50 years post-collapse (Fig. 9). The final stages of ice-shelf collapse may be
 411 preceded years or even decades of gradual weakening (Walker et al., 2024), meaning the
 412 collapse of this unnamed ice shelf at some point between 1963 and 1973 is consistent with
 413 relatively warm environmental conditions in the years or decades earlier and is symbolic of
 414 environmental change in the mid-20th Century.

415



416

417 **Figure 9:** A series of satellite images showing the disintegration of an un-named ice shelf between 1963
 418 and 1973, which has not regrown to a comparable extent in the 50 years since. Satellite images are
 419 courtesy of the U.S. Geological Survey. See Figure 1a for location.

420 The century-long record of surface undulations implies that the ~30-year record of satellite
 421 altimetry is not long enough to capture the full extent of the amplitude and wavelength of
 422 decadal variability in basal-melt anomalies. Numerical-modelling experiments have shown that
 423 forcing Totten Glacier with variable basal-melt rates, at similar amplitudes to those inferred by
 424 ~30 years of satellite-altimetry observations, has a net effect of reducing ice discharge and
 425 delaying grounding-line retreat in comparison to constant forcing (McCormack et al., 2021).



Therefore, evidence of prolonged periods of higher sustained melt rates in the recent past raises the possibility of similar episodes in the coming decades accelerating retreat. A greater understanding of the processes and the magnitude of decadal variability is vital to narrowing uncertainties in future sea-level projections from Antarctica (Hanna et al., 2024). It could be that these anomalous periods of warm oceanic conditions play a vital role in kick starting cycles of glacier retreat. Perhaps analogous to this is Pine Island and Thwaites glaciers, where sediment records point to their retreat from stabilizing pinning points in the 1940s (Clark et al., 2024; Smith et al., 2017) in response to anonymously warm environmental conditions (Steig et al., 2012). The key difference here is that bedrock geometry at Pine Island Glacier was conducive for marine ice-sheet instability and a rapid retreat (Reed et al., 2024), whereas the present geometry at Totten Glacier is not favourable for a similar rapid retreat in the near future (Morlighem et al., 2020).

438

439 5. Conclusion

Overall, our results have shown that averaged decadal ice speed of Totten Ice Shelf has not accelerated over the past half-century. The combination of observations of inland thinning in the earliest satellite-altimetry records, grounding-line retreat between 1973 and 1989, and the absence of any long-term trends in snowfall, points towards Totten Glacier already being out of balance in the 1970s. Therefore, the initial increase in ice discharge that placed Totten Glacier out of balance must have taken place before 1973. The near century-long record of surface-undulation formation highlights an anomalous ~20-year period in the mid-20th century that we interpret as sustained higher-than-average basal-melt rates causing much more limited interaction between a prominent ice rumple near the grounding line and the ice shelf. This interpretation is supported by satellite-altimetry observations that show waves of ice thickness variations travelling with ice flow that match the gap in surface-undulation formation. We hypothesize that these anonymously warm conditions in the mid-20th century could have marked the onset of the modern-day mass loss of Totten Glacier by accelerating the detachment from a key pinning point, and/or marking a change in environmental conditions represented by more frequent and/or intense intrusions of mCDW onto the continental shelf. Validating this proposed anonymously warm period is challenging because the drivers of interannual variability in melt rates at Totten Ice Shelf over the observational period are not fully understood. Perhaps more importantly, because surface undulations have been forming over the past ~30 years, our observations hint at warmer than present conditions in the recent past. Therefore, basal-melt rates calculated from short satellite-altimetry records that are often used as a baseline in numerical models to project into the future may not be capturing the full variability within the Totten glacier system.

462

463

464

465

466

467



468

469 **Data availability:** Landsat and ARGON imagery was provided free of charge by the U.S.
 470 Geological Survey Earth Resources Observation Science Center
 471 (<https://earthexplorer.usgs.gov/>, USGS, 2022). The MOA grounding line product is available
 472 at <https://doi.org/10.7265/N5KP8037> (Haran, 2021). The ice shelf thickness change dataset
 473 from Smith et al. (2020) is available at <http://hdl.handle.net/1773/45388> (last access: April
 474 2022). The REMA DEM is available at <https://doi.org/10.7910/DVN/X7NDNY> (Howat et al.,
 475 2019). ICESat-2 data is available from <https://nsidc.org/data/atl06/versions/6>. Corrected
 476 Landsat imagery of Antarctic ice shelves from 1973 and 1989 is available at
 477 <https://doi.org/10.7488/ds/3810> (Miles and Bingham, 2023). Corrected Argon imagery was
 478 provided by Ron Li. The decadal ice speed tracking vectors and grounding line mapping from
 479 this study are available at <https://doi.org/10.7488/ds/7853>.

480

481 **Acknowledgements:** Bertie W. J. Miles was supported by a Leverhulme Early Career
 482 Fellowship (ECF-2021-484). Tian Li is funded by the European Union's Horizon 2020
 483 research and innovation programme through the project Arctic PASSION (grant number:
 484 101003472). Robert G. Bingham acknowledges funding from NERC (NE/S006613/1).

485

486 **Author Contribution:** B.M led the design of the study with input from T.L and R.B. T.L
 487 produced figure 7a and carried out the ICESat-2 analysis. B.M led the manuscript writing with
 488 input from T.L and R.B

489

490 **Competing interests:** The authors declare that they have no conflict of interest.

491

492 References

- 493 Adusumilli, S., Fricker, H. A., Medley, B., Padman, L., and Siegfried, M. R.: Interannual
 494 variations in meltwater input to the Southern Ocean from Antarctic ice shelves, *Nature*
 495 *Geoscience*, 13, 616-620, 2020.
- 496 Aitken, A. R. A., Roberts, J. L., Ommen, T. D. v., Young, D. A., Gollledge, N. R., Greenbaum,
 497 J. S., Blankenship, D. D., and Siegert, M. J.: Repeated large-scale retreat and advance of
 498 Totten Glacier indicated by inland bed erosion, *Nature*, 533, 385-389, 2016.
- 499 Arthur, J. F., Stokes, C. R., Jamieson, S. S. R., Miles, B. W. J., Carr, J. R., and Leeson, A. A.:
 500 The triggers of the disaggregation of Voyeykov Ice Shelf (2007), Wilkes Land, East
 501 Antarctica, and its subsequent evolution, *Journal of Glaciology*, 67, 933-951, 2021.
- 502 Baumhoer, C. A., Dietz, A. J., Kneisel, C., Paeth, H., and Kuenzer, C.: Environmental drivers
 503 of circum-Antarctic glacier and ice shelf front retreat over the last two decades, *The*
 504 *Cryosphere*, 15, 2357-2381, 2021.
- 505 Bindshadler, R., Vaughan, D. G., and Vornberger, P.: Variability of basal melt beneath the
 506 Pine Island Glacier ice shelf, West Antarctica, *Journal of Glaciology*, 57, 581-595, 2011.



- 507 Brancato, V., Rignot, E., Milillo, P., Morlighem, M., Mouginot, J., An, L., Scheuchl, B., Jeong,
508 S., Rizzoli, P., Bueso Bello, J. L., and Prats-Iraola, P.: Grounding Line Retreat of Denman
509 Glacier, East Antarctica, Measured With COSMO-SkyMed Radar Interferometry Data,
510 Geophysical Research Letters, 47, e2019GL086291, 2020.
- 511 Brunt, K. M., Fricker, H. A., and Padman, L.: Analysis of ice plains of the Filchner–Ronne Ice
512 Shelf, Antarctica, using ICESat laser altimetry, Journal of Glaciology, 57, 965-975, 2011.
- 513 Christie, F. D. W., Bingham, R. G., Gourmelen, N., Tett, S. F. B., and Muto, A.: Four-decade
514 record of pervasive grounding line retreat along the Bellingshausen margin of West
515 Antarctica, Geophysical Research Letters, 43, 5741-5749, 2016.
- 516 Clark, R. W., Wellner, J. S., Hillenbrand, C.-D., Totten, R. L., Smith, J. A., Miller, L. E., Larter,
517 R. D., Hogan, K. A., Graham, A. G. C., Nitsche, F. O., Lehrmann, A. A., Lepp, A. P.,
518 Kirkham, J. D., Fitzgerald, V. T., Garcia-Barrera, G., Ehrmann, W., and Wacker, L.:
519 Synchronous retreat of Thwaites and Pine Island glaciers in response to external forcings
520 in the presatellite era, Proceedings of the National Academy of Sciences, 121,
521 e2211711120, 2024.
- 522 Cook, C. P., Hill, D. J., van de Flierdt, T., Williams, T., Hemming, S. R., Dolan, A. M., Pierce,
523 E. L., Escutia, C., Harwood, D., Cortese, G., and Gonzales, J. J.: Sea surface temperature
524 control on the distribution of far-traveled Southern Ocean ice-rafted detritus during the
525 Pliocene, Paleoceanography, 29, 533-548, 2014.
- 526 Davison, B. J., Hogg, A. E., Slater, T., and Rigby, R.: Antarctic Ice Sheet grounding line
527 discharge from 1996 through 2023, Earth Syst. Sci. Data Discuss., 2023, 1-35, 2023.
- 528 De Rydt, J., Gudmundsson, G. H., Corr, H. F. J., and Christoffersen, P.: Surface undulations
529 of Antarctic ice streams tightly controlled by bedrock topography, The Cryosphere, 7, 407-
530 417, 2013.
- 531 Floricioiu, D. K., L.; Chowdhury, T. A.; Bäessler, M: ESA Antarctic Ice Sheet Climate Change
532 Initiative (Antarctic_Ice_Sheet_cci): Grounding line location for key glaciers, Antarctica,
533 1994-2020, v2.0. NERC EDS Centre for Environmental Data Analysis, 2021.
- 534 Fricker, H. A., Coleman, R., Padman, L., Scambos, T. A., Bohlander, J., and Brunt, K. M.:
535 Mapping the grounding zone of the Amery Ice Shelf, East Antarctica using InSAR,
536 MODIS and ICESat, Antarctic Science, 21, 515-532, 2009.
- 537 Greenbaum, J. S., Blankenship, D. D., Young, D. A., Richter, T. G., Roberts, J. L., Aitken, A.
538 R. A., Legresy, B., Schroeder, D. M., Warner, R. C., van Ommen, T. D., and Siegert, M.
539 J.: Ocean access to a cavity beneath Totten Glacier in East Antarctica, Nature Geoscience,
540 8, 294-298, 2015.
- 541 Greene, C. A., Blankenship, D. D., Gwyther, D. E., Silvano, A., and Van Wijk, E.: Wind causes
542 Totten Ice Shelf melt and acceleration, Science Advances, 3, e1701681-e1701681, 2017.
- 543 Gudmundsson, G. H.: Transmission of basal variability to a glacier surface, Journal of
544 Geophysical Research: Solid Earth, 108, 2003.
- 545 Gwyther, D. E., Galton-Fenzi, B. K., Hunter, J. R., and Roberts, J. L.: Simulated melt rates for
546 the Totten and Dalton ice shelves, Ocean Sci., 10, 267-279, 2014.
- 547 Gwyther, D. E., O’Kane, T. J., Galton-Fenzi, B. K., Monselesan, D. P., and Greenbaum, J. S.:
548 Intrinsic processes drive variability in basal melting of the Totten Glacier Ice Shelf, Nature
549 Communications, 9, 3141, 2018.



- 550 Hanna, E., Topál, D., Box, J. E., Buzzard, S., Christie, F. D. W., Hvidberg, C., Morlighem, M.,
551 De Santis, L., Silvano, A., Colleoni, F., Sasgen, I., Banwell, A. F., van den Broeke, M. R.,
552 DeConto, R., De Rydt, J., Goelzer, H., Gossart, A., Gudmundsson, G. H., Lindbäck, K.,
553 Miles, B., Mottram, R., Pattyn, F., Reese, R., Rignot, E., Srivastava, A., Sun, S., Toller, J.,
554 Tuckett, P. A., and Ultee, L.: Short- and long-term variability of the Antarctic and
555 Greenland ice sheets, *Nature Reviews Earth & Environment*, 5, 193-210, 2024.
- 556 Haran, T., Bohlander, J., Scambos, T., Painter, T. & Fahnestock, M.: MODIS Mosaic of
557 Antarctica 2008-2009 (MOA2009) Image Map. (NSIDC-0593, Version 2). Boulder, C. U.
558 (Ed.), NASA National Snow and Ice Data Center Distributed Active Archive Center, 2021.
- 559 Herraiz-Borreguero, L. and Naveira Garabato, A. C.: Poleward shift of Circumpolar Deep
560 Water threatens the East Antarctic Ice Sheet, *Nature Climate Change*, 12, 728-734, 2022.
- 561 Hirano, D., Tamura, T., Kusahara, K., Fujii, M., Yamazaki, K., Nakayama, Y., Ono, K., Itaki,
562 T., Aoyama, Y., Simizu, D., Mizobata, K., Ohshima, K. I., Nogi, Y., Rintoul, S. R., van
563 Wijk, E., Greenbaum, J. S., Blankenship, D. D., Saito, K., and Aoki, S.: On-shelf
564 circulation of warm water toward the Totten Ice Shelf in East Antarctica, *Nature*
565 *Communications*, 14, 4955, 2023.
- 566 Howat, I. M., Porter, C., Smith, B. E., Noh, M. J., and Morin, P.: The Reference Elevation
567 Model of Antarctica, *The Cryosphere*, 13, 665-674, 2019.
- 568 Jong, L. M., Plummer, C. T., Roberts, J. L., Moy, A. D., Curran, M. A. J., Vance, T. R., Pedro,
569 J. B., Long, C. A., Nation, M., Mayewski, P. A., and van Ommen, T. D.: 2000 years of
570 annual ice core data from Law Dome, East Antarctica, *Earth Syst. Sci. Data*, 14, 3313-
571 3328, 2022.
- 572 Jordan, J. R., Miles, B. W. J., Gudmundsson, G. H., Jamieson, S. S. R., Jenkins, A., and Stokes,
573 C. R.: Increased warm water intrusions could cause mass loss in East Antarctica during
574 the next 200 years, *Nature Communications*, 14, 1825, 2023.
- 575 Khazendar, A., Schodlok, M. P., Fenty, I., Ligtenberg, S. R. M., Rignot, E., and van den Broeke,
576 M. R.: Observed thinning of Totten Glacier is linked to coastal polynya variability, *Nature*
577 *Communications*, 4, 2857, 2013.
- 578 Kim, B.-H., Seo, K.-W., Lee, C.-K., Kim, J.-S., Lee, W. S., Jin, E. K., and van den Broeke, M.:
579 Partitioning the drivers of Antarctic glacier mass balance (2003–2020) using satellite
580 observations and a regional climate model, *Proceedings of the National Academy of*
581 *Sciences*, 121, e2322622121, 2024.
- 582 Kim, S. H., Kim, D.-j., and Kim, H.-C.: Progressive Degradation of an Ice Rumples in the
583 Thwaites Ice Shelf, Antarctica, as Observed from High-Resolution Digital Elevation
584 Models, *Remote Sensing*, 10, 1236, 2018.
- 585 Kusahara, K., Hirano, D., Fujii, M., Fraser, A. D., Tamura, T., Mizobata, K., Williams, G. D.,
586 and Aoki, S.: Modeling seasonal-to-decadal ocean–cryosphere interactions along the
587 Sabrina Coast, East Antarctica, *The Cryosphere*, 18, 43-73, 2024.
- 588 Lee, C.-K., Seo, K.-W., Han, S.-C., Yu, J., and Scambos, T. A.: Ice velocity mapping of Ross
589 Ice Shelf, Antarctica by matching surface undulations measured by ICESat laser altimetry,
590 *Remote Sensing of Environment*, 124, 251-258, 2012.
- 591 Li, R., Cheng, Y., Chang, T., Gwyther, D. E., Forbes, M., An, L., Xia, M., Yuan, X., Qiao, G.,
592 Tong, X., and Ye, W.: Satellite record reveals 1960s acceleration of Totten Ice Shelf in
593 East Antarctica, *Nature Communications*, 14, 4061, 2023a.



- 594 Li, R., Cheng, Y., Cui, H., Xia, M., Yuan, X., Li, Z., Luo, S., and Qiao, G.: Overestimation and
595 adjustment of Antarctic ice flow velocity fields reconstructed from historical satellite
596 imagery, *The Cryosphere*, 16, 737-760, 2022.
- 597 Li, T., Dawson, G. J., Chuter, S. J., and Bamber, J. L.: Grounding line retreat and tide-
598 modulated ocean channels at Moscow University and Totten Glacier ice shelves, East
599 Antarctica, *The Cryosphere*, 17, 1003-1022, 2023b.
- 600 Li, X., Rignot, E., Morlighem, M., Mouginot, J., and Scheuchl, B.: Grounding line retreat of
601 Totten Glacier, East Antarctica, 1996 to 2013. In: *Geophysical Research Letters*,
602 Blackwell Publishing Ltd, 2015.
- 603 Martínez-Botí, M. A., Foster, G. L., Chalk, T. B., Rohling, E. J., Sexton, P. F., Lunt, D. J.,
604 Pancost, R. D., Badger, M. P. S., and Schmidt, D. N.: Plio-Pleistocene climate sensitivity
605 evaluated using high-resolution CO₂ records, *Nature*, 518, 49-54, 2015.
- 606 McCormack, F. S., Roberts, J. L., Gwyther, D. E., Morlighem, M., Pelle, T., and Galton-Fenzi,
607 B. K.: The Impact of Variable Ocean Temperatures on Totten Glacier Stability and
608 Discharge, *Geophysical Research Letters*, 48, e2020GL091790, 2021.
- 609 Miles, B. and Bingham, R.: Landsat mosaics of Antarctic Ice Shelves from 1973 and 1989,
610 1973-1989 [dataset], University of Edinburgh. School of Geosciences., doi:
611 <https://doi.org/10.7488/ds/3810>, 2023. 2023.
- 612 Miles, B. W. J. and Bingham, R. G.: Progressive unanchoring of Antarctic ice shelves since
613 1973, *Nature*, 626, 785-791, 2024.
- 614 Miles, B. W. J., Stokes, C. R., and Jamieson, S. S. R.: Pan-ice-sheet glacier terminus change
615 in East Antarctica reveals sensitivity of Wilkes Land to sea-ice changes, *Science advances*,
616 2, e1501350-e1501350, 2016.
- 617 Miles, B. W. J., Stokes, C. R., Jamieson, S. S. R., Jordan, J. R., Gudmundsson, G. H., and
618 Jenkins, A.: High spatial and temporal variability in Antarctic ice discharge linked to ice
619 shelf buttressing and bed geometry, *Scientific Reports*, 12, 10968, 2022.
- 620 Mohajerani, Y., Velicogna, I., and Rignot, E.: Mass Loss of Totten and Moscow University
621 Glaciers, East Antarctica, Using Regionally Optimized GRACE Mascons, *Geophysical*
622 *Research Letters*, 45, 7010-7018, 2018.
- 623 Morlighem, M., Rignot, E., Binder, T., Blankenship, D., Drews, R., Eagles, G., Eisen, O.,
624 Ferraccioli, F., Forsberg, R., Fretwell, P., Goel, V., Greenbaum, J. S., Gudmundsson, H.,
625 Guo, J., Helm, V., Hofstede, C., Howat, I., Humbert, A., Jokat, W., Karlsson, N. B., Lee,
626 W. S., Matsuoka, K., Millan, R., Mouginot, J., Paden, J., Pattyn, F., Roberts, J., Rosier, S.,
627 Ruppel, A., Seroussi, H., Smith, E. C., Steinhage, D., Sun, B., Broeke, M. R. v. d., Ommen,
628 T. D. v., Wessem, M. v., and Young, D. A.: Deep glacial troughs and stabilizing ridges
629 unveiled beneath the margins of the Antarctic ice sheet, *Nature Geoscience*, 13, 132-137,
630 2020.
- 631 Nakayama, Y., Greene, C. A., Paolo, F. S., Mensah, V., Zhang, H., Kashiwase, H., Simizu, D.,
632 Greenbaum, J. S., Blankenship, D. D., Abe-Ouchi, A., and Aoki, S.: Antarctic Slope
633 Current Modulates Ocean Heat Intrusions Towards Totten Glacier, *Geophysical Research*
634 *Letters*, 48, e2021GL094149, 2021.
- 635 Nakayama, Y., Wongpan, P., Greenbaum, J. S., Yamazaki, K., Noguchi, T., Simizu, D.,
636 Kashiwase, H., Blankenship, D. D., Tamura, T., and Aoki, S.: Helicopter-Based Ocean
637 Observations Capture Broad Ocean Heat Intrusions Toward the Totten Ice Shelf,
638 *Geophysical Research Letters*, 50, e2022GL097864, 2023.



- 639 Nilsson, J., Gardner, A. S., and Paolo, F. S.: Elevation change of the Antarctic Ice Sheet: 1985
640 to 2020, *Earth Syst. Sci. Data*, 14, 3573-3598, 2022.
- 641 Padman, L., Fricker, H. A., Coleman, R., Howard, S., and Erofeeva, L.: A new tide model for
642 the Antarctic ice shelves and seas, *Annals of Glaciology*, 34, 247-254, 2002.
- 643 Paolo, F. S., Fricker, H. A., Padman, L., and Fs Paolo, H. A. F. L. P.: Volume loss from
644 Antarctic ice shelves is accelerating, *Science*, 348, 327-331, 2015.
- 645 Pelle, T., Morlighem, M., Nakayama, Y., and Seroussi, H.: Widespread Grounding Line
646 Retreat of Totten Glacier, East Antarctica, Over the 21st Century, *Geophysical Research*
647 *Letters*, 48, e2021GL093213, 2021.
- 648 Picton, H. J., Stokes, C. R., Jamieson, S. S. R., Floricioiu, D., and Krieger, L.: Extensive and
649 anomalous grounding line retreat at Vanderford Glacier, Vincennes Bay, Wilkes Land,
650 East Antarctica, *The Cryosphere*, 17, 3593-3616, 2023.
- 651 Reed, B., Green, J. A. M., Jenkins, A., and Gudmundsson, G. H.: Recent irreversible retreat
652 phase of Pine Island Glacier, *Nature Climate Change*, 14, 75-81, 2024.
- 653 Ribeiro, N., Herraiz-Borreguero, L., Rintoul, S. R., McMahon, C. R., Hindell, M., Harcourt,
654 R., and Williams, G.: Warm Modified Circumpolar Deep Water Intrusions Drive Ice Shelf
655 Melt and Inhibit Dense Shelf Water Formation in Vincennes Bay, East Antarctica, *Journal*
656 *of Geophysical Research: Oceans*, 126, e2020JC016998, 2021.
- 657 Rignot, E., Mouginot, J., and Scheuchl, B.: Ice flow of the antarctic ice sheet, *Science*, 333,
658 1427-1430, 2011.
- 659 Rignot, E., Mouginot, J., Scheuchl, B., Van Den Broeke, M., Van Wessem, M. J., and
660 Morlighem, M.: Four decades of Antarctic ice sheet mass balance from 1979–2017,
661 *Proceedings of the National Academy of Sciences of the United States of America*, 116,
662 1095-1103, 2019.
- 663 Rintoul, S. R., Silvano, A., Pena-Molino, B., Van Wijk, E., Rosenberg, M., Greenbaum, J. S.,
664 and Blankenship, D. D.: Ocean heat drives rapid basal melt of the totten ice shelf, *Science*
665 *Advances*, 2, 2016.
- 666 Roberts, J., Galton-Fenzi Benjamin, K., Paolo Fernando, S., Donnelly, C., Gwyther David, E.,
667 Padman, L., Young, D., Warner, R., Greenbaum, J., Fricker Helen, A., Payne Antony, J.,
668 Cornford, S., Le Brocq, A., van Ommen, T., Blankenship, D., and Siegert Martin, J.: Ocean
669 forced variability of Totten Glacier mass loss, *Geological Society, London, Special*
670 *Publications*, 461, 175-186, 2018.
- 671 Roberts, J., Plummer, C., Vance, T., van Ommen, T., Moy, A., Poynter, S., Treverrow, A.,
672 Curran, M., and George, S.: A 2000-year annual record of snow accumulation rates for
673 Law Dome, East Antarctica, *Clim. Past*, 11, 697-707, 2015.
- 674 Scambos, T. A., Haran, T. M., Fahnestock, M. A., Painter, T. H., and Bohlander, J.: MODIS-
675 based Mosaic of Antarctica (MOA) data sets: Continent-wide surface morphology and
676 snow grain size, *Remote Sensing of Environment*, 111, 242-257, 2007.
- 677 Schröder, L., Horwath, M., Dietrich, R., Helm, V., van den Broeke, M. R., and Ligtenberg, S.
678 R. M.: Four decades of Antarctic surface elevation changes from multi-mission satellite
679 altimetry, *The Cryosphere*, 13, 427-449, 2019.
- 680 Silvano, A., Rintoul, S. R., Peña-Molino, B., and Williams, G. D.: Distribution of water masses
681 and meltwater on the continental shelf near the Totten and Moscow University ice shelves,
682 *Journal of Geophysical Research: Oceans*, 122, 2050-2068, 2017.



- 683 Smith, B., Fricker, H. A., Gardner, A. S., Medley, B., Nilsson, J., Paolo Nicholas Holschuh, F.
684 S., Adusumilli, S., Brunt, K., Csatho, B., Harbeck, K., Markus, T., Neumann, T., Siegfried,
685 M. R., and Jay Zwally, H.: Pervasive ice sheet mass loss reflects competing ocean and
686 atmosphere processes, *Science*, 368, 1239-1242, 2020.
- 687 Smith, B., Fricker, H. A., Holschuh, N., Gardner, A. S., Adusumilli, S., Brunt, K. M., Csatho,
688 B., Harbeck, K., Huth, A., Neumann, T., Nilsson, J., and Siegfried, M. R.: Land ice height-
689 retrieval algorithm for NASA's ICESat-2 photon-counting laser altimeter, *Remote Sensing*
690 *of Environment*, 233, 111352, 2019.
- 691 Smith, J. A., Andersen, T. J., Shortt, M., Gaffney, A. M., Truffer, M., Stanton, T. P.,
692 Bindshadler, R., Dutrieux, P., Jenkins, A., Hillenbrand, C. D., Ehrmann, W., Corr, H. F.
693 J., Farley, N., Crowhurst, S., and Vaughan, D. G.: Sub-ice-shelf sediments record history
694 of twentieth-century retreat of Pine Island Glacier, *Nature*, 541, 77-80, 2017.
- 695 Steig, E. J., Ding, Q., Battisti, D. S., and Jenkins, A.: Tropical forcing of circumpolar deep
696 water inflow and outlet glacier thinning in the amundsen sea embayment, west antarctica,
697 *Annals of Glaciology*, 53, 19-28, 2012.
- 698 Stokes, C. R., Abram, N. J., Bentley, M. J., Edwards, T. L., England, M. H., Foppert, A.,
699 Jamieson, S. S. R., Jones, R. S., King, M. A., Lenaerts, J. T. M., Medley, B., Miles, B. W.
700 J., Paxman, G. J. G., Ritz, C., van de Flierdt, T., and Whitehouse, P. L.: Response of the
701 East Antarctic Ice Sheet to past and future climate change, *Nature*, 608, 275-286, 2022.
- 702 van Wijk, E. M., Rintoul, S. R., Wallace, L. O., Ribeiro, N., and Herraiz-Borreguero, L.:
703 Vulnerability of Denman Glacier to Ocean Heat Flux Revealed by Profiling Float
704 Observations, *Geophysical Research Letters*, 49, e2022GL100460, 2022.
- 705 Vaňková, I., Winberry, J. P., Cook, S., Nicholls, K. W., Greene, C. A., and Galton-Fenzi, B.
706 K.: High Spatial Melt Rate Variability Near the Totten Glacier Grounding Zone Explained
707 by New Bathymetry Inversion, *Geophysical Research Letters*, 50, e2023GL102960, 2023.
- 708 Walker, C. C., Millstein, J. D., Miles, B. W. J., Cook, S., Fraser, A. D., Colliander, A., Misra,
709 S., Trusel, L. D., Adusumilli, S., Roberts, C., and Fricker, H. A.: Multi-decadal collapse
710 of East Antarctica's Conger–Glenzer Ice Shelf, *Nature Geoscience*, doi: 10.1038/s41561-
711 024-01582-3, 2024. 2024.
- 712 Yamazaki, K., Aoki, S., Katsumata, K., Hirano, D., and Nakayama, Y.: Multidecadal poleward
713 shift of the southern boundary of the Antarctic Circumpolar Current off East Antarctica,
714 *Science Advances*, 7, eabf8755, 2021.
- 715 Ye, W., Qiao, G., Kong, F., Ma, X., Tong, X., and Li, R.: Improved Geometric Modeling of
716 1960s KH-5 ARGON Satellite Images for Regional Antarctica Applications,
717 *Photogrammetric Engineering & Remote Sensing*, 83, 477-491, 2017.
- 718